N91-16700

DISTORTED-WAVE BORN APPROXIMATION CALCULATIONS FOR TURBULENCE SCATTERING IN AN UPWARD-REFRACTING ATMOSPHERE *

Kenneth E. Gilbert, Xiao Di, and Lintao Wang
National Center for Physical Acoustics

University of Mississippi
University, Mississippi

ABSTRACT

Weiner and Keast observed that in an upward-refracting atmosphere, the relative sound pressure level versus range follows a characteristic "step" function. The observed step function has recently been predicted qualitatively and quantitatively by including the effects of small-scale turbulence in a parabolic equation (PE) calculation. [Gilbert *et al.*, J. Acoust. Soc. Am. **87**, 2428-2437 (1990)]. The present paper compares the PE results to single-scattering calculations based on the distorted-wave Born approximation (DWBA). The purpose is to obtain a better understanding of the physical mechanisms that produce the step-function. The PE calculations and DWBA calculations are compared to each other and to the data of Weiner and Keast for upwind propagation (strong upward refraction) and crosswind propagation (weak upward refraction) at frequencies of 424 Hz and 848 Hz. The DWBA calculations, which include only single scattering from turbulence, agree with the PE calculations and with the data in all cases except for upwind propagation at 848 Hz. Consequently, it appears that in all cases except one, the observed step function can be understood in terms of single scattering from an upward-refracted "skywave" into the refractive shadow zone. For upwind propagation at 848 Hz, the DWBA calculation gives levels in the shadow zone that are much below both the PE and the data.

INTRODUCTION

Weiner and Keast[1] and others[2,3] have observed that for sound propagation in an upward-refracting atmosphere, the relative sound-pressure level[4] versus range can be represented as a "step function" (Fig. 1). Recently the observed step function has been predicted qualitatively and quantitatively by parabolic equation (PE) calculations that include the effects of small-scale turbulence.[5]

Figure 2 shows gray-scale plots of the PE calculation without turbulence and with turbulence. The upward-refracted wave is called the "skywave."[6] In the plots with turbulence the skywave is still present although it has been noticeably modified by turbulence. For a

* This work was supported by the Office of Naval Research

source and receiver near the ground, the average relative sound pressure level inside the skywave (region 1 in Fig. 1) is approximately 0 dB (spherical spreading) with or without turbulence. However, the region below the skywave (region 3 in Fig. 1) is dramatically affected by turbulence. Without turbulence a deep shadow zone is predicted by the PE calculation. With turbulence, sound is scattered from the skywave into the shadow zone, producing a relative sound pressure level that is fairly uniform on the average. The region between the skywave and shadow zone (region 2 in Fig. 1) is a transition region. The horizontal extent of region 2 is a strong function of the strength of upward refraction. It is evident that, for a gray-scale plot with turbulence in Fig. 2, a horizontal "cut" through the plot at a particular receiver height will give a step function.

Although the gray-scale plots of the PE calculations give a good qualitative picture for understanding the step function, the PE calculations do not allow a simple physical explanation of the observed quantitative behavior of the relative sound pressure level versus range. For example, what causes the observed constant relative sound pressure level (spherical spreading) at long ranges? In the present paper a simpler calculation is presented which is based on single scattering out of the upward-refracted skywave. The simpler calculation, which uses the distorted-wave Born approximation (DWBA),[7] is compared to the PE calculation and to the data of Weiner and Keast. The objective is to gain insight into the physical mechanisms that produce the observed step function.

I. THEORY

A. Atmospheric model

We want to compare the DWBA calculations to the PE calculations reported in Ref. 5. Hence we use the same atmospheric model as in Ref. 5 and assume that the effects of turbulence can be adequately represented by small fluctuations in the index of refraction. The total index of refraction is thus written as a steady deterministic part $n_d(\vec{R})$ plus a fluctuating stochastic part $\mu(\vec{R},t)$ where $\vec{R} = (x,y,z)$ and t is time. With this approximation for turbulence, the wavenumber is given by

$$k(\vec{R},t) = k_0\left[n_d(\vec{R}) + \mu(\vec{R},t)\right] \quad , \tag{1}$$

where k_0 is a reference wavenumber, $n_d \cong 1$, and $\mu \ll 1$. The deterministic part of the index of refraction n_d is assumed to vary only with the height above the ground z. It was computed from a logarithmic sound-speed profile of the form

$$c_d(z) = \begin{cases} c_0 + a\ ln(z/d), & z \geq z_0 \quad , \\ c_0 + a\ ln(z_0/d) & z < z_0 \quad , \end{cases} \tag{2}$$

where $c_0 = 340$ m/s, $z_0 = 0.01$ m, and $d = 6 \times 10^{-3}$ m. The refraction parameter a is $-.5$ m/s for crosswind propagation (weak upward refraction) and -2.0 m/s for upwind propagation (strong upward refraction). The deterministic parameters were chosen to fit the short-range data of Weiner and Keast.[1]

In the calculations reported here, the fluctuation μ is assumed at any instant of time to be a function of $\vec{R} = (x, y, z)$. In Ref. 5 the turbulence model was two-dimensional so that sound propagated only in the $x - z$ plane. As will be shown, for computing the average sound pressure level using a single scattering approximation, the two atmospheric models are equivalent.

In Ref. 5 the stochastic wavenumber in Eq. (1) was used directly to calculate "snapshots" of the acoustic field. Here, we want to compute average levels so we need the autocorrelation function for μ. The autocorrelation function is defined by

$$C(\vec{S}) \equiv \langle \mu(\vec{R} + \vec{S})\mu(\vec{R}) \rangle \quad , \tag{3}$$

where $\langle\rangle$ denotes an ensemble average over many realizations of μ. (We assume an ensemble average and time average are equivalent.) For small-scale turbulence near the ground, $C(\vec{S})$ can be approximated by a Gaussian autocorrelation function of the form

$$C(\vec{S}) = \mu_0^2 e^{-(S_x^2/l_x^2 + S_y^2/l_y^2 + S_z^2/l_z^2)} \quad , \tag{4}$$

where μ_0 is the root-mean-square value of μ, and l_x, l_y, and l_z are the correlation lengths in the x, y and z directions, respectively. In numerical calculations isotropic turbulence was assumed ($l_x = l_y = l_z = l$). The input values for μ_0 and l ($\mu_0 = 1.42 \times 10^{-3}$, and $l = 1.1$ m) were taken from measurements reported by Daigle.[8]

B. Ground impedance model

The ground was modeled as a flat, locally reacting plane with an angle-independent complex impedance. Impedance values were obtained from the empirical formulas of Delaney and Bazley[9] using an effective flow resistivity of 300 rayls/cm. The resulting impedance values were $7.19 + i8.20$ and $5.17 + i5.57$ at 424 Hz and 848 Hz, respectively.

C. Distorted-wave Born approximation (DWBA) calculations

We consider a point source with angular frequency ω in a turbulent atmosphere. At a particular instant in time the solution for a point source (Green's function) in a turbulent atmosphere satisfies

$$\nabla^2 G(\vec{R}, \vec{R}') + k_0^2(n_d + \mu)^2 G(\vec{R}, \vec{R}') = -4\pi\delta(\vec{R} - \vec{R}') \quad , \tag{5}$$

where $\vec{R}'$ is the source location, and $\vec{R}$ is the receiver location. In the absence of turbulence ($\mu = 0$) the Green's function G_0 is given by

$$\nabla^2 G_0(\vec{R}, \vec{R}') + k_0^2 n_d^2 G_0(\vec{R}, \vec{R}') = -4\pi\delta(\vec{R} - \vec{R}') \quad , \tag{6}$$

where G_0 is a refracted wave (i.e., a distorted wave) if n_d varies with height. In this section we shall consider both an undistorted spherical wave and a wave distorted by upward refraction.

An integral equation for G which goes to G_0 in the absence of turbulence can be written as

$$G(\vec{R},\vec{R}') = G_0(\vec{R},\vec{R}') + \frac{1}{4\pi}\int G_0(\vec{R},\vec{R}'')\delta k^2(\vec{R}'')G(\vec{R}'',\vec{R}')d^3\vec{R}'' \quad , \tag{7}$$

where $\delta k^2 = k_0^2(n_d+\mu)^2 - k_0^2 n_d^2 \cong 2\mu k_0^2$, since $n_d \cong 1$ and $\mu \ll 1$.

Equation (7) allows us to write the total solution, G, as the solution in the absence of turbulence, G_0, plus an integral which gives the turbulent contribution. However, since the unknown G appears in the integral, Eq.(7) is as difficult to solve exactly as is the original differential equation. When δk^2 is "small enough" the full solution G that appears in the integral can be approximated by G_0. The approximation $G \cong G_0$ is generally known as the "Born approximation". When G_0 is a refracted wave the approximation is often called the "distorted-wave Born approximation" or "DWBA."[7]

Writing the turbulent contribution as δG , using $G \cong G_0$, and $\delta k^2 \cong 2\mu k_0^2$ we have

$$\delta G = \frac{k_0^2}{2\pi}\int G_0(\vec{R},\vec{R}'')\mu(\vec{R}'')G_0(\vec{R}'',\vec{R}')d^3\vec{R}'' \quad . \tag{8}$$

We want to calculate the time average of $|G|^2$, which we assume is the same as an ensemble average. Denoting the average value of $|G|^2$ as $\langle|G|^2\rangle$ and assuming a random phase between G and δG we have

$$\langle| G |^2\rangle = \langle| G_0 |^2\rangle + \langle| \delta G |^2\rangle \quad , \tag{9}$$

where

$$\begin{aligned}\langle| \delta G |^2\rangle = \frac{k_0^4}{4\pi^2}\int G_0^*(\vec{R},\vec{R}''')G_0^*(\vec{R}''',\vec{R}')\langle\mu(\vec{R}''')\mu(\vec{R}'')\rangle \\ \times G_0(\vec{R},\vec{R}'')G_0(\vec{R}'',\vec{R}')d^3\vec{R}'''d^3\vec{R}'' \quad .\end{aligned} \tag{10}$$

Now $\langle\mu(\vec{R}''')\mu(\vec{R}'')\rangle = C(\vec{S})$ where C is the autocorrelation function and $\vec{S} = \vec{R}''' - \vec{R}''$. Transforming from the variables ($\vec{R}''$, $\vec{R}'''$) to the variables ($\vec{R}''$, $\vec{S}$) gives

$$\begin{aligned}\langle| \delta G |^2\rangle = \frac{k_0^4}{4\pi}\int G_0^*(\vec{R},\vec{R}''+\vec{S})G_0^*(\vec{R}''+\vec{S},\vec{R}')C(\vec{S}) \\ \times G_0(\vec{R},\vec{R}'')G_0(\vec{R}'',\vec{R}')d^3\vec{S}\ d^3\vec{R}'' \quad .\end{aligned} \tag{11}$$

For the sake of illustration we first consider an undistorted spherical wave in free space, i.e., we take $G_0(\vec{R},\vec{R}'') = \exp(ik_0|\vec{R}-\vec{R}''|)/|\vec{R}-\vec{R}''|$. For $|\vec{R}'| = 0$ (source at the origin) and $|\vec{R}''| >> |\vec{S}|$, the Green's function $G_0(\vec{R}''+\vec{S},\vec{R}'=0)$ can be approximated as

$$G_0(\vec{R}''+\vec{S},\vec{R}'=0) \cong \frac{e^{ik_0|\vec{R}''|}}{|\vec{R}''|}e^{i\vec{k}\cdot\vec{S}} \quad , \tag{12}$$

where the $\vec{k} = k_0\hat{n}$, and $\hat{n} = (\vec{R}''/|\vec{R}''|)$. Similarly the Green's function $G_0(\vec{R},\vec{R}''+\vec{S})$ can be approximated as

$$G_0(\vec{R},\vec{R}''+\vec{S}) \cong \frac{e^{ik_0|\vec{R}-\vec{R}''|}}{|\vec{R}-\vec{R}''|}e^{-i\vec{k}'\cdot\vec{S}} \quad , \tag{13}$$

where $\vec{k}' = k_0\hat{n}'$, and $\hat{n}' = (\vec{R}-\vec{R}'')/|(\vec{R}-\vec{R}'')|$. With these approximations for the free-space Green's functions, we have

$$\langle| \delta G |^2\rangle = \frac{k_0^4}{4\pi^2}\int \frac{1}{|\vec{R}''|^2}\frac{1}{|\vec{R}-\vec{R}''|^2}e^{i(\vec{k}'-\vec{k})\cdot\vec{S}}C(\vec{S})d^3\vec{S}d^3\vec{R}'' \quad . \tag{14}$$

We now define a scattering function $\sigma(\vec{q})$ as

$$\sigma(\vec{q}) \equiv \int e^{i\vec{q}\cdot\vec{S}}C(\vec{S})d^3\vec{S} \quad , \tag{15}$$

where $\vec{q} = \vec{k}' - \vec{k}$. Then Eq. (14) becomes

$$\langle| \delta G |^2\rangle = \frac{k_0^4}{4\pi^2}\int \frac{1}{|\vec{R}''|^2}\sigma(\vec{q})\frac{1}{|\vec{R}-\vec{R}''|^2}d^3\vec{R}'' \quad . \tag{16}$$

In Eq. (16) we can identify $1/|\vec{R}''|^2$ as the sound intensity I_{inc} incident on the scattering volume and $1/|\vec{R}-\vec{R}''|^2$ as the scattered intensity I_{scat} that reaches the receiver. Hence we can write

$$\langle| \delta G |^2\rangle = \frac{k_0^4}{4\pi^2}\int I_{inc}(\vec{R}'')\sigma(\vec{q})I_{scat}(\vec{R}'')d^3\vec{R}'' \quad . \tag{17}$$

Equation (17) has a useful physical interpretation (see Fig. 4). The average intensity of the sound reaching the receiver from a particular volume of space is proportional to the product of the incident intensity reaching the volume, the scattering strength of the volume, and the scattered intensity. The Appendix gives an analytic result for Eq. (17) for small-angle scattering.

In order to take upward refraction into account we use the following prescription: In Eq. (17) we replace the incident intensity $I_{inc} = 1/|\vec{R}''|^2$ and the scattered intensity $I_{inc} = 1/|\vec{R} - \vec{R}''|^2$ with $I_{inc} = |G_{PE}(\vec{R}'')|^2$ and $I_{scat} = |G_{PE}(\vec{R}, \vec{R}'')|^2$, respectively, where G_{PE} denotes the Green's function without turbulence computed using the parabolic equation method described in Refs. 5 and 10. Writing the integrals in Cartesian coordinates we have

$$\begin{aligned}\langle | \delta G |^2 \rangle &= \frac{k_0^4}{4\pi^2} \int | G_{PE}(\vec{R}'')^2 \mid G_{PE}(\vec{R}, \vec{R}'') |^2 \\ &\times \exp\left[i(q_x S_x + q_y S_y + q_z S_z)\right] C(S_x, S_y, S_z) dx'' dy'' dz'' dS_x dS_y dS_z \quad .\end{aligned} \tag{18}$$

Since G_{PE} is azimuthally symmetric and $|\vec{R}''| >> |\vec{S}|$, we neglect the y-dependence in G_{PE} and integrate $\exp(iq_yS_y)$ over y and obtain the δ-function result obtained in the Appendix. (See Eqs. (A2) - (A4).) Also we set $q_x = 0$, as in the Appendix, and obtain

$$\begin{aligned}\langle | \delta G |^2 \rangle &= \frac{1}{x} \frac{k_0^3}{2\pi} \int x''(x - x'') \mid G_{PE}(\vec{R}'') |^2 | G_{PE}(\vec{R}, \vec{R}'') |^2 \\ &\times e^{iq_z S_z} C(S_x, 0, S_z) dS_x dS_z dx'' dz'' \quad .\end{aligned} \tag{19}$$

Using the general Gaussian autocorrelation function in Eq.(4) for the integrations over S_x and S_z, we have

$$\begin{aligned}\langle | \delta G |^2 \rangle &= \frac{\mu_0^2 k_0^3 l_x l_z}{2x} \int x''(x - x'') \mid G_{PE}(x'', z'') |^2 \\ &\times | G_{PE}(x, z; x'', z'') |^2 \, e^{-q_z^2 l_z^2/4} dx'' dz'' \quad .\end{aligned} \tag{20}$$

In the parabolic equation method the quantity actually solved for is $\Psi(r, z)$, where $G_{PE}(r, z) = [\exp(ik_0 r)/\sqrt{r}\ ]\Psi(r, z)$, and $r = \sqrt{x^2 + y^2}$. Since the integral is now two-dimensional, we can set y to zero and let $r = x$. Then in terms of $\Psi(x, z)$ we have

$$\begin{aligned}\langle | \delta G |^2 \rangle &= \frac{\mu_0^2 k_0^3 l_x l_z}{2x} \int | \Psi(x'', \ z'') |^2 | \Psi(x - x''; z, z'') |^2 \\ &\times e^{-q_z^2 l_z^2/4} dx'' dz'' \quad .\end{aligned} \tag{21}$$

In the numerical calculations we assumed the turbulence to be isotropic with a correlation length l. Hence we have finally

$$\begin{aligned}\langle | \delta G |^2 \rangle &= \frac{\mu_0^2 k_0^3 l^2}{2x} \int | \Psi(x'', z''); \ z, \ z'' |^2 | \Psi(x - x''; z, z'') |^2 \\ &\times e^{-q_z^2 l^2/4} dx'' dz'' \quad ,\end{aligned} \tag{22}$$

where x'' goes from zero to x, and z'' goes from zero to infinity.

II. NUMERICAL CALCULATIONS

A. Comparison of DWBA calculations with PE calculations and with experiment

In Fig. 3 the DWBA calculations and the PE calculations are compared to each other and to the data of Weiner and Keast. The data is for octave bands of random noise between 300-600 Hz and 600-1200 Hz, respectively. In both the DWBA and the PE calculations, the frequency was taken to be $\sqrt{f_1 f_2}$ where f_1 and f_2 are the lowest and highest frequencies, respectively, in the octave bands considered. Section I gives the parameters for the atmospheric model and the ground impedance model used in the calculations. Note that the DWBA calculations and the data are for the average relative sound pressure level while the PE calculations are a "snapshot" of the relative sound-pressure level and not the average level. However, the trend in a particular PE calculation is generally fairly close to the average level predicted by the corresponding DWBA calculation.

The DWBA calculations, which include only single scattering from turbulence, give a good approximation to the average PE levels in all cases except for upwind propagation at 848 Hz. For upwind propagation at 848 Hz, the DWBA prediction deep in the shadow zone is much below both the PE and the data.

B. Discussion of numerical results

Some of the features of the curves in Fig. 3 can be understood in a straightforward way using the DWBA calculations. The deterministic (no turbulence) part of the Green's function is G_0 and the stochastic part due to turbulence is δG. Near the source (regions 1 and 2 in Fig. 1) we have $| G_0 |^2 \gg \langle | \delta G |^2 \rangle$ while at long ranges (region 3 in Fig.1) we have just the reverse. Consequently, near the source, the shape of a given curve for relative sound pressure level versus range is governed by the deterministic sound-speed profile so the level is essentially what one would obtain from a calculation without turbulence.

Since we have $| G_0 |^2 \ll \langle | \delta G |^2 \rangle$ at long range, the relative sound pressure level is due almost entirely to scattering from turbulence. In order to understand the long-range behavior of the curves in Fig. 3 we must make a more detailed analysis than was required at short range. As shown in the Appendix, the contribution to the relative sound pressure level from turbulence scattering in free space (with no refraction) diverges as the logarithm of the range. We expect similar behavior even with upward refraction over a finite impedance plane. Consider the situation in Fig. 4 where we have a scattering volume with an incident intensity I_{inc} and a scattered intensity I_{scat}. The sound intensity incident on the scattering volume is proportional to $1/r^2$ where r is the horizontal range to the receiver. The scattering volume itself is proportional to r^3. The scattered intensity reaching the receiver from the scattering volume, like the incident intensity, is proportional to $1/r^2$. For a fixed scattering angle, the average scattered intensity from the volume is thus proportional to $(1/r^2) \times (r^3) \times (1/r^2) = 1/r$. Hence, as shown in Eq. (A9), we expect the relative sound pressure level to increase as the logarithm of the horizontal range. This behavior at long range is seen in the DWBA calculation for crosswind propagation (weak upward refraction) at 424 Hz. When there is significant upward refraction the height of the scattering volume is not proportional to the range but increases more rapidly than linearly with range. As a result, the scattering angle is not fixed but increases with increasing range. Since the scattered intensity is reduced at larger scattering angles, the relative sound pressure level versus range is "flattened" so that a nearly constant relative sound pressure level is reached at long ranges. Because of the flattening effect caused by an increasing scattering angle, a nearly constant relative sound pressure level is seen in the DWBA calculation for upwind propagation (strong upward refraction) at 424 Hz. A similar behavior is seen for crosswind propagation (weak upward refraction) at 848 Hz. The flattening effect with weak upward refraction at 848 Hz is apparently due to the greater sensitivity to the scattering angle at the higher frequency.

The DWBA calculation for upwind propagation (strong upward refraction) at 848 Hz falls off in the shadow zone much more rapidly than the PE calculation and the data. The major computational difference between the two calculations is that the PE calculation includes multiple scattering while the DWBA calculation does not. Hence the disagreement indicates that for upwind propagation at 848 Hz, multiple scattering is important. This interpretation is supported by a gray-scale plot for this case which shows the skywave greatly modified by turbulence so that the approximation $G \cong G_0$ is not valid.

III. SUMMARY AND CONCLUSIONS

We have compared distorted-wave Born approximation (DWBA) calculations to parabolic equation (PE) calculations and to the data of Wiener and Keast. In all cases except one, the DWBA calculations, which include only single scattering, predicted the step-function behavior of the relative sound pressure level versus range seen in both the data and the PE calculations. The important conclusion to be reached is that, in the presence of upward refraction, single scattering can give a relative sound pressure level that does not diverge as the logarithm of the range but rather is nearly constant at long range. Hence, in all cases except one, the observed step function can be understood in terms of single scattering from an upward-refracted skywave.

For upwind propagation (strong upward refraction) at 848 Hz, the DWBA calculation grossly underestimated both the data and the PE calculation. In this case, the single scattering approximation $G \cong G_0$ was not valid in the skywave. To accurately predict multiple scattering of sound into the shadow zone, one must have a good predictive model for sound propagation in the skywave itself. Hence, it would be valuable to have measurements not only for the sound scattered into the refractive shadow, but also for the sound field in the skywave.

APPENDIX: ANALYTIC EXPRESSION FOR FREE-SPACE SCATTERING FROM ANISOTROPIC TURBULENCE

To see the general behavior of Eq. (17) we can consider weak small-angle scattering in free space . For weak small-angle scattering we can use the Born approximation and obtain an analytic result for anisotropic turbulence.

For small angle scattering we can let $1/|\vec{R}''|^2 \cong 1/x''^2$ and $1/|\vec{R} - \vec{R}''|^2 \cong 1/(x - x'')^2$. We could integrate Eq. (17) directly using a particular autocorrelation function such as a Gaussian. However, to obtain a more general result that does not assume any particular autocorrelation function, it is convenient to return to the form in Eq. (14) which is written in terms of the autocorrelation function $C(S_x, S_y, S_z)$,

$$\begin{aligned} \langle | \delta G |^2 \rangle = & \frac{k_0^4}{4\pi^2} \int \frac{1}{x''^2} \frac{1}{(x - x'')^2} e^{i(q_x S_x + q_y S_y + q_z S_z)} \\ & C(S_x, S_y, S_z)\, dx''\, dy''\, dz''\, dS_x\, dS_y\, dS_z \quad . \end{aligned} \tag{A1}$$

For small angles we can approximate q_z as

$$\begin{aligned} q_z & \cong k_0 \left(\frac{1}{x''} + \frac{1}{x - x''}\right) z'' \\ & = k_0 \left[\frac{x}{x''(x - x'')}\right] z'' \quad . \end{aligned} \tag{A2}$$

Similarly,

$$q_y \cong k_0 \left[\frac{x}{x''(x - x'')}\right] y'' \quad . \tag{A3}$$

We now consider the integral over z'':

$$\begin{aligned} \int_{-\infty}^{+\infty} e^{iS_z k_0 [x/x''(x - x'')] z''}\, dz'' = & \; 2\pi\, \delta \left[k_0 \frac{x}{x''(x - x'')} S_z\right] \\ = & \; \frac{2\pi}{k_0} \frac{x''(x - x'')}{x} \delta(S_z) \quad . \end{aligned} \tag{A4}$$

The integral over y'' gives a similar result with S_z replaced by S_y. Inserting the results from integrating over z'' and y'' into Eq. (A1) and integrating over S_z and S_y, we have

$$\langle | \delta G |^2 \rangle = \frac{k_0^2}{x^2} \int e^{iq_x S_x} C(S_x, 0, 0)\, dx''\, dS_x \quad . \tag{A5}$$

We could integrate over S_x and define a special scattering function

$\sigma_{00} = \int C(S_x, 0, 0) \exp(iq_x S_x) dS_x$. However, we are considering small-angle propagation. Hence $\vec{q}$ is almost perpendicular to the propagation direction and we can therefore set q_x to zero. Thus, integrating in the region between the source and receiver we have

$$\begin{aligned} \langle | \delta G |^2 \rangle &= \frac{k_0^2}{x^2} \int_{-\infty}^{\infty} C(S_x,\ O,\ O)\ dS_x \int_0^x dx'' \\ &= \frac{k_0^2}{x} C_{00} \quad , \end{aligned} \tag{A6}$$

where

$$C_{00} = \int_{-\infty}^{\infty} C(S_x,\ O,\ O) dS_x \quad . \tag{A7}$$

For anisotropic turbulence having a Gaussian autocorrelation function (See Eq.(4)) we obtain

$$\langle | \delta G |^2 \rangle = \sqrt{\pi}\ \mu_0^2\, k_0^2\, l_x / x \quad . \tag{A8}$$

Thus for weak small-angle scattering in free space, the scattering due to turbulence falls off inversely with the range and depends on the correlation length only in the direction of propagation. Note that, written in terms of the relative sound pressure level (RSPL), the contribution from turbulence scattering diverges as the logarithm of the range.

$$\begin{aligned} RSPL &= 10 \log_{10} (x^2 \langle | \delta G |^2 \rangle) \\ &= 10 \log_{10} (\sqrt{\pi} \mu_0^2\, k_0^2\, l_x) + 10 \log_{10} (x) \quad . \end{aligned} \tag{A9}$$

REFERENCES

1. F. M. Weiner and D. N. Keast, "Experimental study of the propagation of sound over ground," J. Acoust. Soc. Am. **31**, 724-733 (1959).

2. P. H. Parkin and W. E. Scholes, "The horizontal propagation of sound from a jet engine close to the ground at Radlett," J. Sound. Vib. **1** (4), 1-13 (1964).

3. P. H. Parkin and W. E. Scholes, "The horizontal propagation of sound from a jet engine close to the ground at Hatfield," J. Sound.Vib. **2** (4), 353-374 (1965).

4. Reference 1 above reports the negative of the relative sound pressure level (excess attenuation). The relative sound pressure level in Ref. 1 is the level corrected for spherical spreading and atmospheric absorption and adjusted to be O dB at 30.5 m (100 ft.). We assume this level is the same as the sound pressure level relative to a free field.

5. K. E. Gilbert, R. Raspet, and X. Di, "Calculation of turbulence effects in an upward refracting atmosphere," J. Acoust. Soc. Am. **87**, 2428-2437 (1990).

6. J.E. Piercy, T.F.W. Embleton, and L.C. Sutherland, "Review of noise propagation in the atmosphere, " J. Acoust. Soc. Amer. **61**, 1403-1418 (1977).

7. L. S. Rodberg and Roy M. Thaler, *Introduction to the Quantum Theory of Scattering* (Academic Press, New York, 1967).

8. G.A. Daigle, "Effects of atmospheric turbulence on the interference of sound waves above a hard boundary," J. Acoust. Soc Amer. **64**, 622-630 (1978).

9. M.E. Delany and E.N. Bazley, "Acoustical properties of fibrous absorbent materials," Appl. Acoust. **3**, 105-116 (1970).

10. K.E. Gilbert and M.J. White, "Application of the parabolic equation to sound propagation in a refracting atmosphere," J. Acoust. Soc. Amer. **85**, 630-637 (1989).

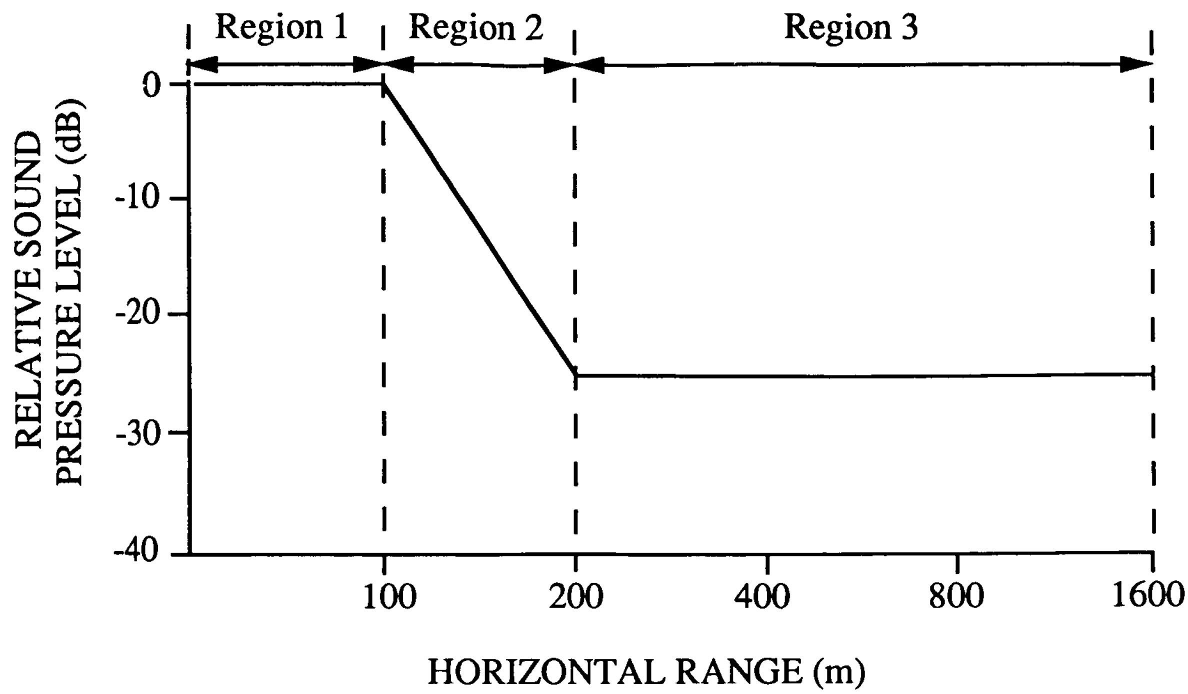

Fig. 1. Characteristic "step" function for the relative sound pressure level versus range for sound propagation in an upward-refracting atmosphere. (From Gilbert et al.[5])

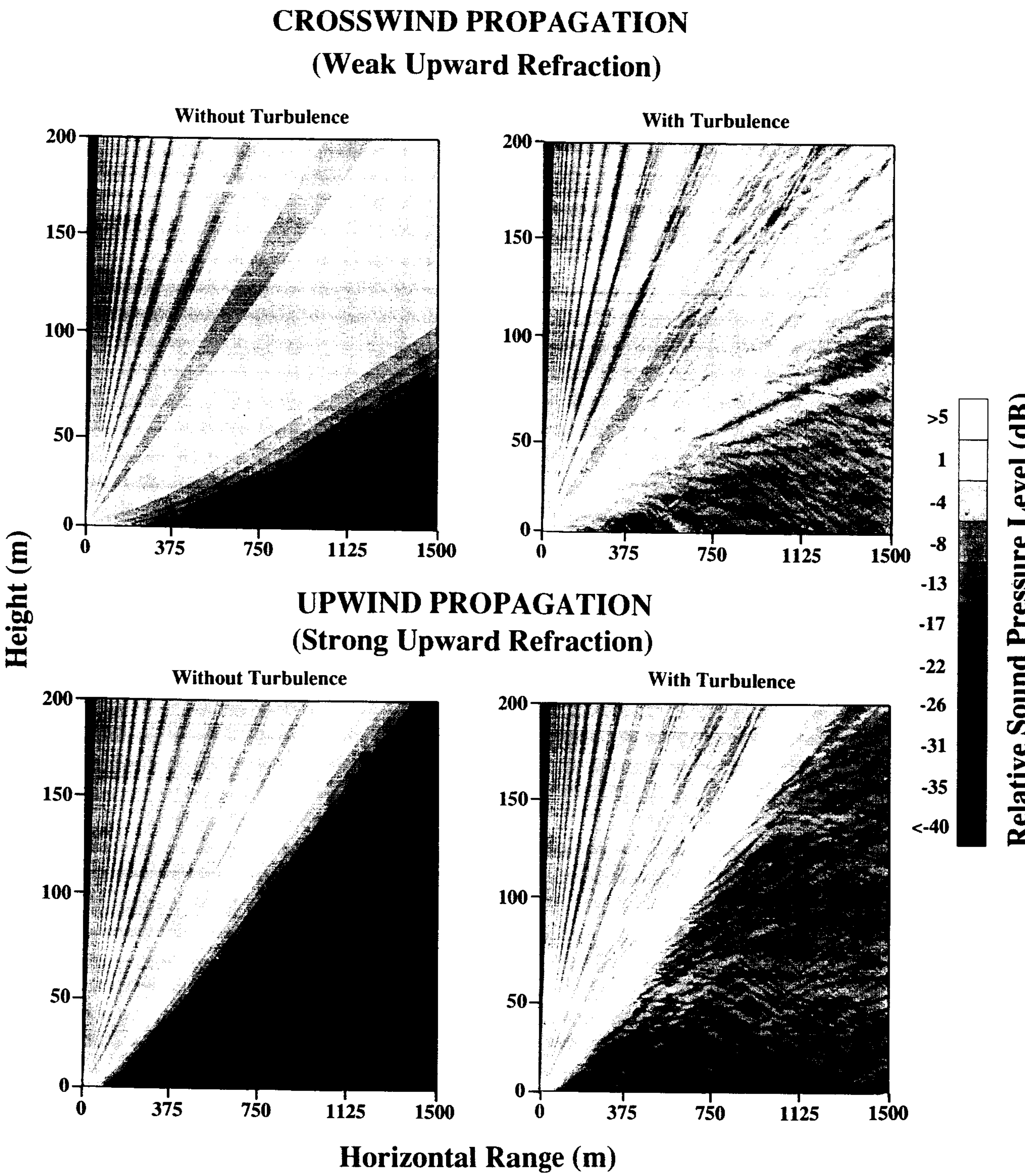

Fig. 2. Gray-scale plots of relative sound pressure level versus height and horizontal range for a non-turbulent atmosphere and a turbulent atmosphere. The frequency is 424 Hz, and the source height is 3.7 m (12 ft). Parameters for the atmospheric model and ground impedance model are given in the text. (From Gilbert et al.[5])

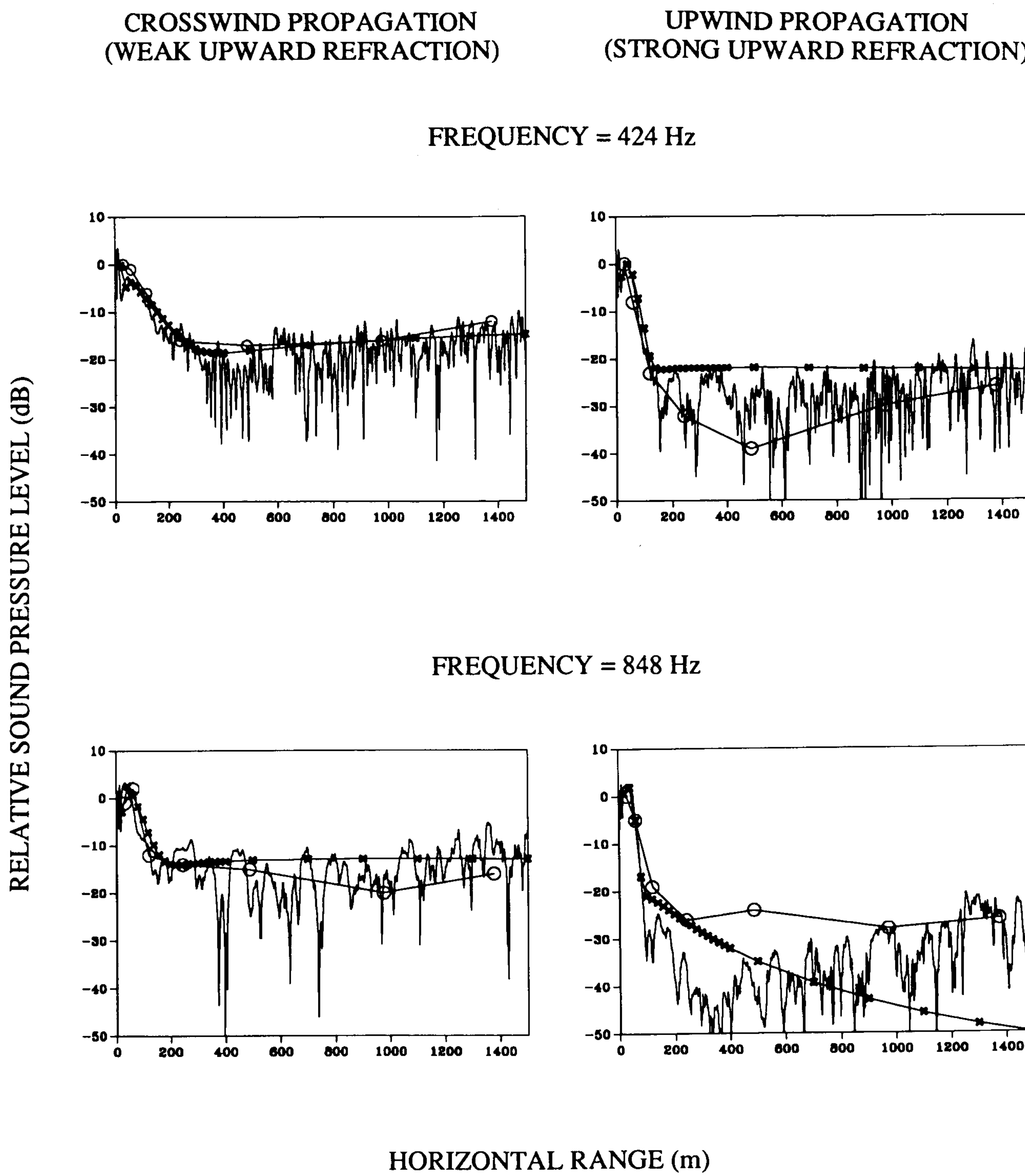

Fig. 3. Relative sound pressure level versus horizontal range for a refracting, turbulent atmosphere. The connected circles are the data of Weiner and Keast.[1] The solid lines are parabolic equation results from Ref. 5. The connected x's are distorted-wave Born approximation calculations. Parameters for the atmospheric model and ground impedance model are given in the text.

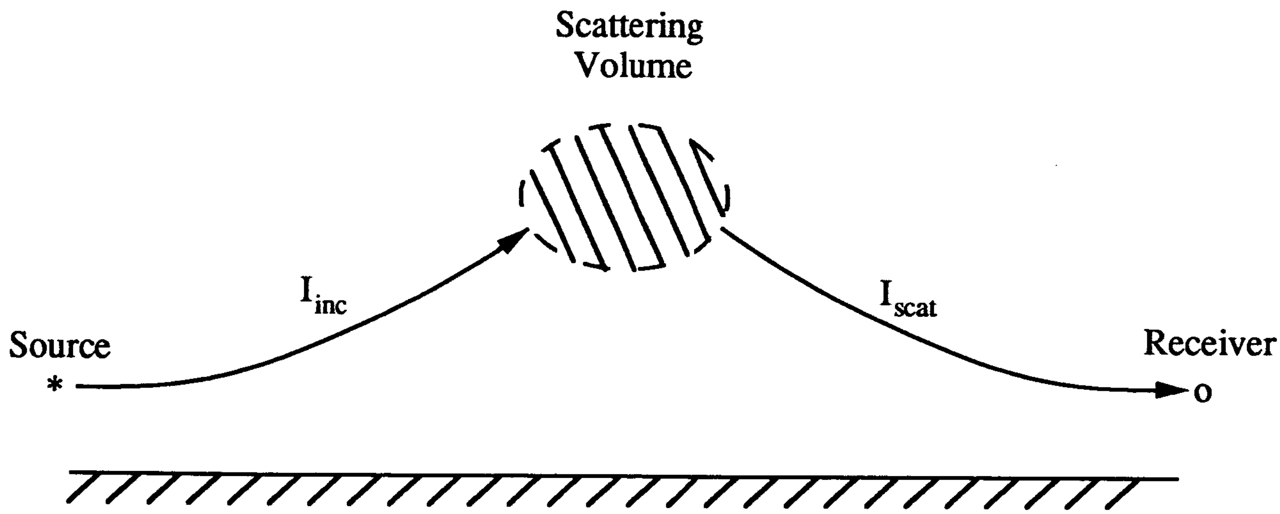

Fig. 4. Schematic representation of scattering from turbulence. The quantity I_{inc} is the average intensity incident on a particular scattering volume, and I_{scat} is the average scattered intensity. The total scattered intensity is obtained by integrating over the volume between the source and receiver.